Interplay of Physical Structure and Photophysics for a Liquid Crystalline Polyfluorene

M. Grell,*,† D. D. C. Bradley,† G. Ungar,‡ J. Hill,† and K. S. Whitehead†

Department of Physics and Astronomy, The University of Sheffield, Hicks Building, Hounsfield Rd, Sheffield S3 7RH, UK, and Department of Engineering Materials, The University of Sheffield, Sir Robert Hadfield Building, Mappin Street, Sheffield S1 3JD, UK

Received May 12, 1999; Revised Manuscript Received July 7, 1999

ABSTRACT: From photophysical evidence, we suggest a structural model based on intrachain ordering that can account for the changes of the absorption spectrum of poly(9,9-dioctylfluorene) (PFO) films under certain physicochemical treatment protocols. We correlate this model to the results of X-ray fiber diffraction experiments.

1. Introduction

There are a number of features of organic semiconductors, including solution processability, band gap tuning by chemical structure, and self-organization, that make them very attractive as potential replacements for conventional inorganic semiconductors. The discovery of electroluminescence (EL) in a polymer semiconductor[1] has led to intensive research in this field, and progress is documented in several recent reviews.[2]

Most attention to date has focused on precursor-route poly(*p*-phenylenevinylene) (PPV)[3] and its soluble derivatives.[4] Recently, however, polyfluorenes[5a] have emerged as attractive alternatives, and they have become the subject of considerable attention.[6−22] Poly(9,9-dioctylfluorene) (PFO), **1**, for example, is a high-

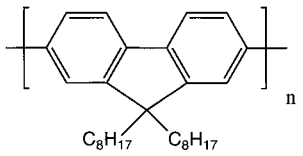

1

mobility hole transport polymer[6] from which efficient blue EL devices have been fabricated.[7] The physicochemical properties of polyfluorenes can be tailored via side chain substitution without substantially changing the electronic properties of the backbone.[8] Band gap and energy level engineering, on the other hand, can be readily achieved via copolymerization.[5b,9,10]

Another interesting feature of polyfluorenes is their liquid crystallinity.[10−14] It has been shown that PFO[11] and fluorene copolymers[10] display liquid crystalline (LC) phases with high order parameters[12] above their melting points and at temperatures that are well below those for thermal decomposition. These phases were found to align readily into monodomains.[10,11] The latter feature allowed fabrication of an EL device that emits highly polarized light[13] and that is consequently of potential for use as a backlight for LC display devices.[14]

In this paper, we will address another physicochemical feature of PFO that strongly affects photophysical properties. In two recent publications,[15,16] we have reported on dramatic changes in the absorption spectra of PFO that result from certain treatment protocols. For example, an additional absorption peak can be induced at the long wavelength edge of the $\pi-\pi^*$ absorption band by dissolving PFO in a moderately poor solvent such as cyclohexane. The new peak appears at $\lambda = 437 \pm 1$ nm and slowly grows in intensity over periods of several hours but without any shift in position. In parallel with the additional absorption band, solutions in cyclohexane undergo a thermally reversible gelation when stored at room temperature for a few days.[16] For spin-coated thin films, exposure to solvent vapors (e.g., toluene and tetrahydrofuran (THF)) or a thermal cycle in which the film is cooled to liquid nitrogen temperature and then slowly reheated to room temperature leads to a very similar additional absorption peak.[15,16] For comparison, thermal crystallization of PFO results in an additional shoulder at the red flank of the absorption spectrum[11] but no additional peak.

Here, we report on physicochemical, photophysical, and X-ray investigations to determine the structure underlying these spectroscopic phenomena, and we discuss the mechanism leading to that structure.

2. Results and Discussion

2.1. Physical Chemistry and Photophysics. In addition to our previous reports, we have found gelation and formation of an additional absorption peak for PFO dissolved in α-pinene, a chiral solvent with a similar solubility parameter to that of cyclohexane. Exposure of films to hexane and cyclohexane (but not methanol) vapor also produces the long wavelength absorption peak. In the case of films cooled to liquid nitrogen temperature and then reheated to room temperature, we observe that the additional peak appears during *reheating* and only for moderately slow heating rates (≤1 °C/min). A combination of vapor exposure and multiple cooling/heating cycles can lead to an additional absorption peak with a relative height of some 50% of that of the original 384 nm $\pi-\pi^*$ absorption peak of untreated, as spin-coated PFO films. This is clearly shown in Figure 1. The additional peak always remains very narrow (fwhm 15 nm) and possesses a vibronic progression that is superimposed on the original $\pi-\pi^*$ absorption peak.

† Department of Physics and Astronomy.
‡ Department of Engineering Materials.
* Author for correspondence.

10.1021/ma990741o CCC: $18.00
Published on Web 08/13/1999

Table 1. PL Emission Peak Wavelengths (and Shoulders (s)) for PFO after Different Treatments: In Solution (0.1 g/L in Toluene); Spin-Coated Film without Further Treatment; Film Quenched (Rapidly Cooled) from 200 °C; Film Crystallized under Nitrogen; Film Crystallized under Air; Film of Gelled Solution (α-Pinene) Smeared onto a Substrate; Film Exposed to THF Vapor at 40 °C; Film Cooled to 77 K/Slowly Reheated to Room Temperature[a]

toluene soln*	as spin-coated*	quench	crystal(N_2)	crystal(Air)	gelled/smeared	THF vapor	liq N_2	MeLPPP
420	426	430	433	433	440	441	439	463
441	446	452	455	457	466	468	466	497
475 (sh)	485	487	490	490	500	500	498	532
505 (s)	518	520	522	522	535	539	534	568 (s)
	560 (s)	560 (s)	570 (s)	560 (s)	572 (s)	582 (s)	580 (s)	

[a] Excitation was at 420 nm (*excitation at 390 nm). Shoulder locations have a margin of error of ±10 nm. For comparison, the data for a methyl-substituted ladder-type poly(*p*-phenylene) (MeLPPP) film[30] are shown in the last column.

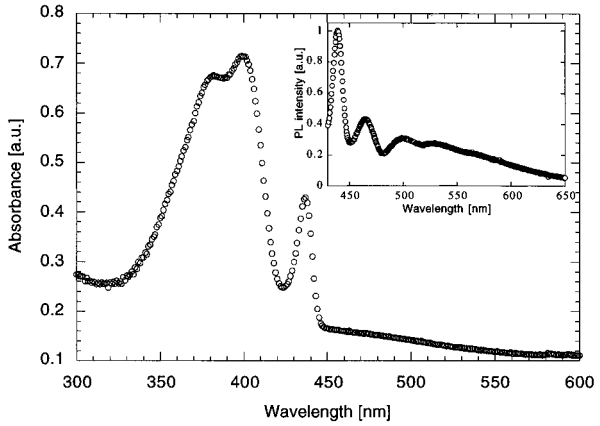

Figure 1. Absorption spectrum of a PFO film that has been cooled to 77 K/reheated to room temperature, exposed to toluene vapor for 60 h, and cooled/reheated four more times. Note the additional absorption peak at 437 nm which is absent in freshly spin-coated or quenched films. The inset shows the PL emission of a vapor-exposed film (excitation at 420 nm).

We have further observed that the formation of an additional absorption peak in cyclohexane solution depends on concentration. The additional peak is observed, and gelation occurs in a 10 g/L solution[16] but not in more dilute (≤1 g/L) solutions. Behavior in solution is more sensitive to the precise conditions (solvent quality, concentration) than the behavior of solid films exposed to solvent vapors.

To study the impact of physicochemical state on PFO photoluminescence (PL) properties, we compare the location of PL emission peaks of PFO in different states in Table 1. "Quenched" and "crystallized" films were produced via suitable thermal treatment protocols,[11] as described in the Experimental Section. Columns six, seven, and eight present results for samples that show the additional 437 nm absorption peak.

Table 1 shows a continuous red shift of spectra in the sequence "solution" to "as spin-coated" to "quenched" to "crystallized". This is as expected for both the effect of an increasing dielectric constant due to densification and the effect of an increasing effective conjugation length due to better ordering of the polymer backbone. All three methods for introducing an additional absorption peak (gelling in poor solvent, exposure to THF vapor, cooling to liquid N_2 temperature, and reheating) result in PL spectra red-shifted by some 15−20 nm from the spectrum of an "as spin-coated" sample.

We note that under specific experimental conditions (e.g., prolonged exposure to heat under air) the PL spectra can show an additional broad, featureless band which is red-shifted by some 100 nm from the shortest wavelength peak of the original emission. This is reminiscent of excimer[24] fluorescence. Bliznyuk et al.[25] explain this excimer band as the result of partial thermooxidative degradation. Note that even when there has been rather little degradation, drastic changes in the PL spectrum can still occur due to efficient energy migration:[26] The PL spectrum is much more sensitive to impurities and defects than absorption spectra are. However, the additional absorption peak we discuss here is not the result of degradation. The additional peak could always be removed, and the behavior of a glassy sample was recovered by heating into the melt and subsequent quenching.[11] An excimer band in PL cannot be removed in this way. We have avoided the conditions leading to chemical degradation by applying a nitrogen atmosphere when necessary, and we shall not discuss degradation-related phenomena any further in this paper.

We speculated previously[16] that the additional peak could be associated with a particular form of *intra*chain order, namely, a well-defined sequence of dihedral angles between subsequent repeat units that leads to a fully extended chain conformation. To investigate this hypothesis, we have studied the behavior of dilute blends of PFO in polystyrene (PS). Interchain contacts can be reduced by increasing dilution, while intrachain ordering should not be affected. We have prepared films by spin-coating from solutions of (30%, 10%, 1%) PFO/(70%, 90%, 99%) PS (wt/wt) in toluene. Spin-coating very quickly removes solvent, and although PFO and PS are probably not thermodynamically compatible, the resulting glassy film will have had little chance to phase separate. We believe that this situation applies particularly to the 1% PFO/PS blend. A freshly spin-coated 1% PFO/PS film was annealed at 90 °C, i.e., above the T_g of PFO (≈75 °C[11]) but below the T_g of PS (105 °C[27]), for 18 h. Figure 2 shows its absorption spectrum (a) compared to a control sample of pure PFO (b) subjected to an identical annealing protocol. The control sample shows a long wavelength shoulder typical of semicrystalline samples.[11] A very similar result was found for a 30% PFO/PS sample (not shown here). No shoulder, however, is found in the absorption spectrum of the dilute 1% PFO/PS sample. The absence of crystallization for this film is in contrast to both the pure PFO and 30% PFO/PS samples and provides compelling evidence that the PFO is in fact molecularly dispersed in the PS at this concentration. For higher concentrations of PFO in PS this is not the case.

For every dilution investigated, including the 1% PFO/PS composition, an additional peak was observed after vapor exposure and also after cooling to 77 K and slowly reheating to room temperature. The thermal stability of the additional peak is improved for the highest dilution (Figure 3). None of the additional absorption peaks' intensity is lost until the glass transition temperature of the PS matrix (105 °C) is reached.

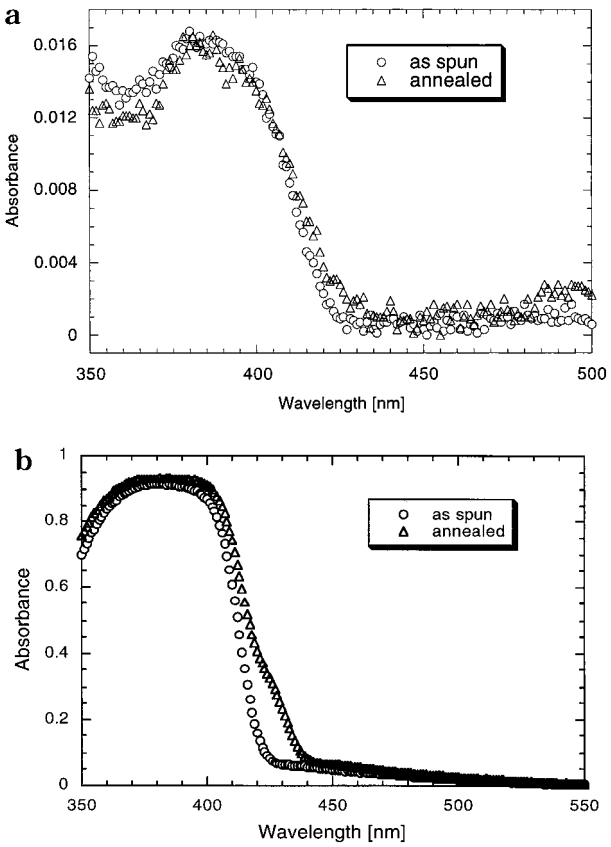

Figure 2. Absorption spectra of (a) a 1% PFO/PS film in the as spin-coated state and after annealing for 18 h at 90 °C and of (b) a control sample 100% PFO as spin-coated and after identical thermal treatment. Open circles, as spin-coated; open triangles, annealed. A very similar result to that in (b) was found for a 30% PFO/PS sample.

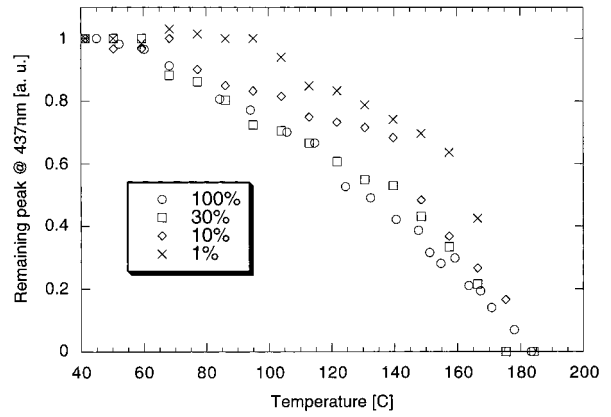

Figure 3. Remaining intensity of additional peak (normalized to initial intensity of additional peak) vs temperature. Heating scans at 2.5 °C/min. Data for 100% PFO were taken from ref 16.

This stabilization for the 1% PFO in PS composition is again consistent with a molecular dispersion of PFO within the glassy PS matrix. For 10% and 30% PFO in PS, no stabilization is observed, and we conclude that at these concentrations phase separation takes place during film preparation.

Figure 4 shows the kinetics of formation for the additional peaks, parametric in the PFO concentration. The relative intensity (peak at 437 nm/main peak at 384 nm) after 24 h of vapor exposure is *enhanced* for the most dilute PFO/PS blend. If one accepts that spin-coating from a 1% PFO/PS solution leads to a film

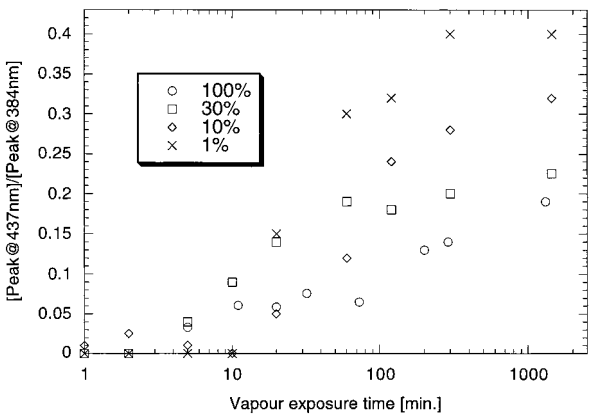

Figure 4. Relative intensity of additional peak (normalized to 384 nm peak) vs vapor exposure time for pure PFO film (100%) and three films of PFO diluted in PS (30%/10%/1% PFO content).

Table 2. PL Emission Peak and Shoulder (s) Wavelengths for Films of PFO Diluted in a PS Matrix, Treated by Cooling to Liquid N_2 Temperature/Reheating, or Exposure to THF Vapor at 40 °C[a]

30% PFO liq N_2	30% PFO THF	10% PFO liq N_2	10% PFO THF	1% PFO liq N_2	1% PFO THF
442	442	438	438	438	438
466	466	464	464	466	463
497	500	498	499	499	499
533	537	530	532	532	537
585 (s)	585 (s)	585 (s)	585 (s)	?	?

[a] Shoulder locations have a margin of error of ±10 nm. For 1% PFO/PS, PL is too weak to assign shoulder values.

containing molecularly dispersed PFO, then the observation that the additional peak can still be introduced rules out an interchain origin. We note further that interchain aggregation in conjugated polymers generally results in emission spectra with much stronger red shifts than reported here[28] or even in spectra dominated by a broad, featureless aggregate band.[23,24] Unlike the additional peak in PFO, aggregate absorption is often weak and is unambiguously confirmed only by PL excitation spectroscopy[23,28] (but not always[24]). Furthermore, site selective fluorescence spectroscopy reveals a localization effect for direct excitation of the aggregate.[23] In the samples investigated here, however, no change is observed in the emission spectrum even when the additional absorption peak is excited directly.

Table 2 lists the positions of the PL peaks of dilute PFO in PS after the cooling/reheating and vapor exposure treatments. All peak positions are very close to those of pure PFO films with the additional absorption peak (compare with last three columns of Table 1) and are essentially independent of dilution. Again, this is consistent with an intrachain ordering.

The similarity between the photophysical properties of ladder-type poly(*p*-phenylenes) (LPPPs)[23,29,30] and PFO films with the additional absorption peak is intriguing. The absorption spectra of different LPPPs typically peak between 441[23] and 463 nm[30] with several well-resolved vibronic replicas spaced by ≈1400 cm^{-1}. The PL spectra have a mirror image relation to the absorption spectra and have Stokes shifts[23,30] of 180−500 cm^{-1}. For comparison, difference absorption spectra for PFO samples before and after treatment show the additional peak at 437 ± 1 nm with two well-resolved vibronic replicas.[15] The PL spectrum is a mirror image of the difference spectrum[15,16] and has its short wave-

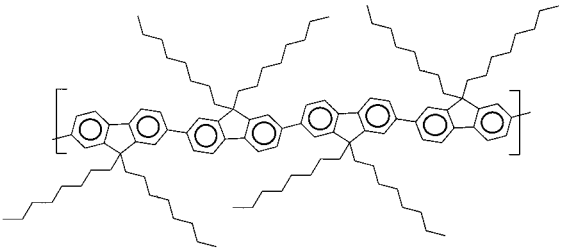

Figure 5. A fully extended PFO chain segment, adopting the "planar zigzag" or 2_1 helix conformation.

length maximum at 441 ± 1 nm. The resulting Stokes shift is calculated to be 210 ± 100 cm^{-1}. The large error margin results from not using the more accurate site-selective fluorescence measurement[23] to determine the Stokes shift. From the seventh column in Table 1 we compute a vibronic spacing of approximately 1400 cm^{-1}.

We note that, under all treatments that lead to an additional absorption peak, the PFO chains are subject to stress, of either mechanical or thermodynamic origin. During the cooling/reheating treatment protocol, a mismatch between substrate and film thermal expansion coefficients will lead to mechanical stress in the PFO film. The additional peak will only form if the heating rate is slow enough that a transfer of mechanical stress between substrate and film can occur rather than slip. On exposure to solvent vapors, PFO films will swell, leading to a swelling stress.[31] Hexane, although a nonsolvent for PFO, will still be a swelling agent due to its compatibility with the aliphatic side chains. The polar methanol, however, will not swell PFO, and consequently no additional peak is produced. Interestingly, for 1% PFO/PS films exposed to toluene vapor, we found a relatively enhanced additional absorption peak as compared to the case of pure PFO (but not for PFO/PS blends of higher PFO concentration, Figure 4). We concluded above that PFO is molecularly dispersed in PS for 1% PFO/PS blends. As a consequence, it will experience the swelling stress of the PS matrix which for the good PS solvent toluene[27] may well be higher than for pure PFO.

We propose that, as a response to this mechanical stress, PFO chains adopt an extended conformation, which can be approximately described as "planar zigzag" or 2_1 helix; see Figure 5. The fact that the emerging peak at 437 nm does not shift in position indicates that this process results in very long extended chain segments without intermediate states. The growth in additional peak intensity with exposure time reflects the increasing number of elongated chain segments.

PFO in the all-planar, 2_1 helical backbone conformation is structurally very similar to LPPPs with their chemically fixed, planar backbones. This explains the similarity of the photophysics between PFO with additional absorption peak and LPPPs.

It is known, however, that in the case of oligo(*p*-phenylenes) (PPPs) the phenyl rings cannot adopt a fully coplanar arrangement due to the steric repulsion of the substituents of neighboring rings. Instead, successive ring planes are rotated by a twist angle of 23° for unsubstituted oligo-*p*-phenylenes and up to 45° for side-chain-substituted PPPs.[32] There is little doubt that an analogous mechanism will also oppose planarization and hence the adoption of a 2_1 helical arrangement in PFO. It should be noted, however, that for PFO with its noncollinear arrangement of phenylene rings[16] the 2_1 helical arrangement is elongated compared to a random conformation. This elongation will help to reduce the mechanical stress. Consequently, planarization is a response of the system in accordance with Le Chatelier's principle.[33] This is not the case for PPPs, where planarization will not help to reduce the mechanical stress. However, other forms of backbone ordering are conceivable which will also result in elongated chain conformations. These will have longer structural repeat units than two monomers. The fully planarized conformation shown in Figure 5 may well be an oversimplification, which in reality is approached only to a limited degree.

We note that, in contrast to the vapor-treated films, thermally crystallized PFO films only show a shoulder at the "red" edge of the absorption spectrum (ref 11 and Figure 2b). We regard this feature as a "precursor" of the fully developed additional peak. This observation suggests that the length of the ordered segments in thermally crystallized PFO is shorter than that in vapor-exposed PFO.

The situation in solution is more intricate, and we have observed that formation of the additional peak depends critically on solvent quality[15,16] and concentration. We exclude polymer/solvent compound formation with subsequent gelation, because it usually is observed only in good solvents.[34] Here, gelation is not observed in any good solvent (toluene, THF, chloroform) but does occur in moderatly poor solvents (cyclohexane,[15] α-pinene). Berghmans et al. have shown that the gelation of syndiotactic PMMA in toluene[35] and *o*-xylene[36] is the result of helical intrachain ordering and subsequent interchain aggregation of helical segments. They found the first, intramolecular step even in solutions that are too dilute for subsequent gelation. In contrast, the formation of an additional absorption peak in PFO/cyclohexane solutions requires a minimum concentration. Consequently, we attribute the additional absorption peak of PFO/cyclohexane gels to solution crystallization, a process that is typically concentration and solvent quality driven. We suggest that in solution crystallized PFO the backbone adopts the same conformation as in vapor-exposed films, with a longer correlation length than for thermal crystallization.

2.2. X-ray Scattering. To arrive at additional structural information on PFO in its different physicochemical states, we have carried out fiber diffraction X-ray scattering experiments. The resulting diffraction patterns are shown in Figure 6: part a is for a glassy fiber quenched from the liquid crystalline state. Part b is for the same fiber subsequently annealed at 140 °C to induce thermal crystallization. Part c is for a second quenched fiber that was exposed to toluene vapor for 3 days at 40 °C. Vapor-exposed fibers show a color change from pale to intense yellow, which is a visual indication for the formation of the additional absorption peak. Finally, part d is for the solvent-exposed fiber after it was subsequently annealed at 135 °C. Note that the fiber axis is always vertical.

The diffraction patterns in Figure 6 show considerable differences in the degree of order and in diffraction coherence length between samples prepared in different ways. These parameters, extracted from diffraction line broadening, are given in Table 3. Where there is a notable increase in line width with increasing scattering angle, the contributions to line broadening from strain and finite crystal size (through the Scherrer equation[37]) were deconvoluted. Lattice strain was otherwise ne-

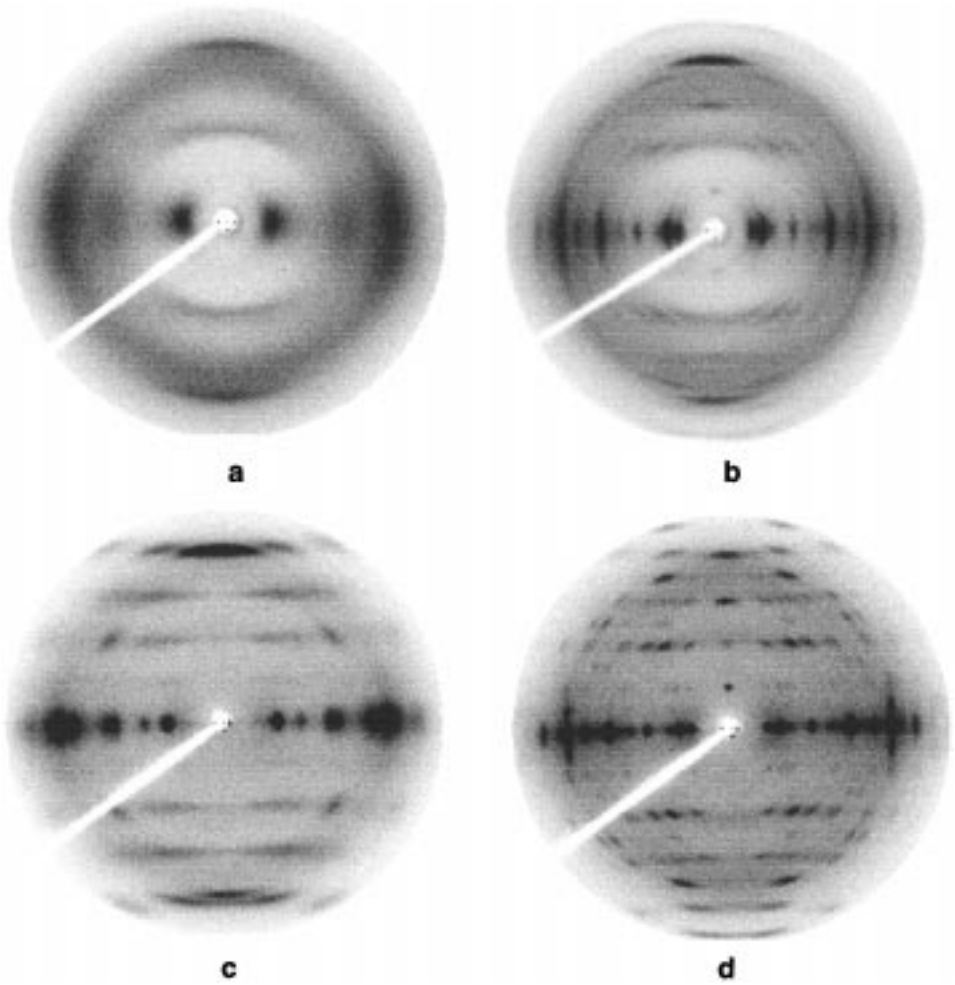

Figure 6. Diffraction from PFO fibers (fiber axis vertical) after the following treaments: (a) fiber drawn from liquid crystalline melt; (b) same fiber as (a), after thermal crystallization (140 °C, 1 h); (c) fiber exposed to saturated toluene vapor (40 °C, 3 days); (d) same fiber as (c) after subsequent annealing (135 °C, 1 h).

Table 3. Structural Data for PFO Fibers after Different Physicochemical Treatments[a]

structural parameters from X-ray data	as-drawn, quenched (nematic glass) (a)	as (a) plus annealed at 140 °C for 1 h (α-form) (b)	as (a) plus vapor exposure (β-form) (c)	as (c) plus annealed at 135 °C for 1 h (α-form) (d)
measurement temperature (°C)	25	140	25	135
coherence length normal to fiber (Å)	35	200	400	500
coherence length parallel to fiber (Å)	80	150	220	400
lattice strain (%) normal to fiber		0.6	1.5	0.5
lattice strain (%) parallel to fiber		0	0	0.2
orientation distribution half-width (deg)	13	8	3	2.5

[a] For (c), the fiber was exposed to saturated toluene vapor at 40 °C for 3 days to allow for complete diffusion. For modifications b, c, and d, the coherence lengths given are the average crystallite dimensions normal/parallel to the chain backbone.

glected. In the case of diffuse scattering from the nematic fiber, the coherence lengths quoted are good approximations of correlation lengths in the sense of the Scherrer equation.

The diffraction pattern in Figure 6a for the quenched glassy fiber shows only diffuse scattering along both the equator and the meridian. The pattern is typical of a nematic liquid crystal with its director pointing along the fiber axis. A quenched fiber is a nematic glass and reflects the state of the polymer during high-temperature fiber drawing. There are two major equatorial scattering maxima centered at scattering angles corresponding to Bragg spacings of 16 and 4.4 Å. They indicate local, i.e., short-range, biaxiality in the stacking of ribbonlike molecules. The "ribbons" imply an anisometric cross section of the averaged polymer chain, the "width" (16 Å) being significantly greater than the "thickness" (4.4 Å). Unlike the more conventional "hairy rod" polymers, where side chains emanate from the aromatic backbone roughly coplanar,[38,39] the side chains in PFO are perpendicular to the aromatic plane. Hence, it is expected that the width of the ribbons would be roughly parallel to the alkyl side chains but normal to the fluorene plane. The width should thus be close to the combined length of the two *n*-octyl groups, i.e., 21 Å. The corresponding measured spacing of only 16 Å suggests that the octyl chains are tilted relative to the direction of edge-to-edge stacking of the ribbons. The high-intensity 4.14 Å meridional maximum is assigned to the stacking of the octyl side chains in the direction of the polymer backbone. However, the spacing between adjacent side chain attachment sites along an individual

backbone is twice that distance (8.3 Å). It is therefore envisaged that neighboring polymer backbones must be displaced along their length by half a monomer unit (4.15 Å) relative to each other. This allows for intercalation of side chains and more efficient space filling. We suggest that this different type of side chain packing may be correlated with the unusual ability of PFO and related polymers to undergo thermotropic alignment into monodomain structures on rubbed substrates.[10,11,13] This behavior is crucial for the potential application of PFO and related polymers for polarized EL devices.[13] In this context, it will be interesting to investigate the alignment properties of novel hairy-rod type PPP polymers, which recently have been found to have noninterdigitating side chains.[39]

The parallel-to-fiber coherence length of the glassy liquid crystalline fiber is 80 Å (Table 3), comparable to the persistence length, $l_p = {}^1/_2 l_{Kuhn} = 85.5 \pm 10.5$ Å, of PFO chains in dilute THF solution.[16] This indicates that there is little difference of the backbone conformation between a dissolved PFO chain and a chain in the liquid crystalline melt.

Figure 6b shows the effect of thermal crystallization. This treatment results in what we shall term the α-phase crystal structure. The crystallinity is reflected in the appearance of several sharp diffraction arcs. Also, the intrachain coherence length is almost doubled as compared to the liquid crystalline state (150 vs 80 Å). We regard this as the result of the ordering of the chain backbone into a specific conformation which is effective in compensating for the bend of the monomer unit, i.e., ensuring that the para-axes of the first ring of subsequent structural repeat units are parallel (note that the structural repeat unit is not necessarily the chemical repeat unit). The simplest conformation that is capable of achieving such a compensation is the 2_1 helical arrangement discussed earlier. However, the α-phase is characterized by a fiber repeat (= crystallographic unit cell length) of 33.4 Å, equal to four monomer units. Many backbone arrangements with a repeat unit of four monomers which do compensate for the fluorene bend are conceivable, and these do not necessarily imply a fully planarized chain backbone. Although the results of our crystallographic study currently in progress are not yet available, we can say that the increased intrachain coherence length proves an ordering of the chain backbone into an elongated conformation, and we suggest that this improved elongation is responsible for the shoulder at the "red" flank of the absorption spectrum for thermally crystallized PFO films.

If instead of being heat-treated the quenched nematic fiber is exposed to toluene vapor for 3 days at 40 °C, another crystal modification is obtained. We refer to this as the *β*-phase (Figure 6c).

The *β*-phase has a fiber periodicity of 16.6 Å, equal to the length of two monomer units and half the periodicity of the α-phase. As already discussed, this does not necessarily imply a different chain backbone conformation to that of the α-phase. A backbone structural repeat length of four chemical repeat units can result in an apparent fiber repeat length equivalent to only two chemical units if the registry between neighboring chains is poor. In terms of the paracrystal theory,[40] this would be described by high cross-terms g_{13} and g_{23} of the lattice distortion tensor. Such interchain slippage in the *β*-phase is evidenced in Figure 6c by the horizontal streaking of the meridional diffraction into layer lines. This slippage of chains should not be confused with the normal-to-fiber correlation length that is in fact higher for the *β*-phase than for the thermally crystallized α-phase (see Table 3). This correlation length, however, refers to the regularity of chain spacing only, not to interchain slippage. Since photophysical interchain phenomena will normally not extend far beyond nearest neighbors (with the notable exception of Förster transfer), the degree of interchain slippage may well be more important for the interpretation of spectra than the normal-to-fiber correlation length.

Notably, in the *β*-phase obtained by the present procedure, in spite of the interchain slippage, the intrachain correlation length is longer than for the thermally crystallized fiber in the α-phase (220 vs 150 Å). That means that the chain backbone ordering is improved. From our photophysical observations, we recall that a vapor-exposed film showed an additional absorption peak instead of the additional shoulder of the thermally crystallized sample. We conclude again that the degree of *intra*chain, not *inter*chain, ordering governs the photophysical properties and that a longer intrachain correlation results in a longer effective conjugation length that gives rise to the additional peak. Figure 6c also reveals an enhanced degree of chain orientation for the *β*-phase fiber. The half-width at half-maximum (hwhm) of the azimuthal distribution of crystalline reflections is only 3° (see Table 3). This reflects an excellent alignment of chains parallel to the fiber axis, which again implies a backbone arrangement that compensates for the bend of the fluorene unit.

The diffraction pattern of the fiber in the *β*-phase changes little with increasing temperature until between 110 and 120 °C, where there is a transformation to the α-phase. The α-phase crystalline fiber thus obtained is highly oriented, with orientational hwhm of only 2.5° (Figure 6d and Table 3) and an intrachain correlation length of 500 Å. This is more than half the contour length of the typical PFO chain (peak molecular weight relates to 116 chemical repeat units,[16] i.e., approximately 900 Å contour length). Also, the layer lines of Figure 6c have elvolved into resolved spots, indicating improved interchain registry. In an additional spectroscopic experiment, we have found that the additional absorption peak for a thin film is preserved on the thermal transition from the *β*-phase to the α-phase. We are hence led to believe that the chain backbone arrangements in the α- and *β*-phase are the same, and the differences in photophysics are based on intrachain correlation lengths only.

Good correlation exists between the appearance of the additional absorption peak and the degree of orientational order of the crystals (azimuthal hwhm; Table 3). Thus, a clearly resolved additional absorption peak is observed in the spectra of both the *β*- and α-phase in the vapor-exposed polymer, both of which are highly oriented. In contrast, the α-phase obtained by thermal crystallization is less well oriented and only has an absorption shoulder.

Overall, the route to achieving the highest degree of both positional and orientational order, starting from a melt-drawn quenched fiber, is the two-stage process of solvent vapor exposure followed by a thermal anneal. We believe that the observed changes of spectroscopic properties are the consequence of an increased degree of backbone order as quantified by the coherence lengths parallel to the fiber in Table 3. It is known in general

that the effective conjugation length[3] of a conjugated polymer can be limited (deliberately) by conformational defects.[41] On the other hand, for "infinitely" long segments the effective conjugation length will be limited intrinsically. We believe that for PFO we have observed the transition from a conformationally to an intrinsically limited conjugation length via enhanced backbone ordering.

Klärner and Miller[17] have investigated a homologous series of dihexylfluorene oligomers in solution and conclude that the length of the effectively conjugated segment in a poly(dihexylfluorene) sample is 11.8 repeat units, i.e., ≈100 Å. Their analysis is based on a linear extrapolation of the absorption maxima vs $^1/_n$, where n is the number of repeat units. This approach is known to be problematic, especially for large n, and Klärner and Miller suggest a limiting absorption maximum of only 403 nm for $n \rightarrow \infty$. This falls significantly short of the observed position of the additional absorption peak found at 437 nm for PFO. It appears therefore that 11.8 repeat units represents a conformationally limited effectively conjugated segment length. Klärner and Miller's investigation appears to amount to an alternative determination of the persistence length of intrachain-disordered (dissolved) polyfluorene. We have determined the same quantity by coupled GPC/light scattering to be 85.5 ± 10.5 Å,[16] which within the experimental error overlaps with Klärner and Miller's result. Only for highly intrachain ordered polyfluorene is the intrinsic limit for effective conjugation approached.

3. Conclusions

Spectroscopic properties of conjugated polymers can have varying degrees of sensitivity to backbone conformation. In poly(*p*-phenylenes) (PPPs), effective conjugation is limited by a twist between neighboring rings. This is more pronounced for longer side chains and is accompanied by a blue shift of absorption and emission.[32] This observation has motivated the synthesis of ladder-type poly(*p*-phenylenes) (LPPPs) which have no degree of conformational freedom. Spectral changes due to physicochemical state are then the result of aggregation or other *inter*molecular phenomena.[29] In poly(*p*-phenyleneethynylene)s (PPEs) rotations of phenylene rings with respect to each other are possible. These do not, however, affect spectroscopic properties because the cylindrically symmetric ethynylene bonds effectively mediate conjugation regardless of the rings' relative orientations.[24] In poly(*p*-phenylenevinylenes) (PPVs)[42] ring torsions can occur about the phenylene to vinylene single bond. In addition, substituents can influence the vinylene bond angle, opening it out beyond the ideal 120°. Further complications arise from the influence of cis and trans configurations of the vinylene double bond and from higher order sequences, e.g., trans-transoid vs trans-cisoid, etc. The precursor route chemistry is also prone to cross-linking side reactions and incomplete conversion (either deliberate or unintentional) which leads respectively to branched or segmented (with saturated spacers) conjugation.

For PFO, we have demonstrated that, via suitable physicochemical treatment protocols in the solid state, we can arrive at highly intrachain ordered polyfluorene. Improved intrachain order results in a much longer effective conjugation length which leads to the observed spectroscopic changes.

4. Experimental Section

All solvents used where HPLC grade products from Aldrich. Synthesis of polyfluorene (PFO) is described elsewhere.[5a] After synthesis, the resulting polymer was reacted with benzene boronic acid to convert the terminal bromine groups into phenyl end groups. The bromine content was thus reduced to typically 5−20 ppm. The PFO used here has an absolute peak molecular weight of 45 000, which corresponds to 116 repeat units per chain.[16] Films of PFO and PFO in PS were spin-coated from 10 g/L solutions in toluene (20 g/L in the case of 1% PFO/PS) at 2000 rpm. To quench, samples were rapidly cooled from 200 °C to room temperature; to crystallize, films were cooled from 200 °C to room temperature at a rate of 1 °C/min under N_2 atmosphere or air, as specified. These procedures are based on our previously reported thermophysical investigations.[11] Vapor exposure was in a covered glass dish immersed in a solvent reservoir thermalized at 40 °C. Cooling/heating cycles were carried out on the coldfinger of an evacuated cryostat that was cooled by liquid nitrogen. Absorption spectroscopy was carried out in a UNICAM 4 UV/vis spectrophotometer. PL was excited with the emission of a GaN diode, filtered through a 420 nm band-pass interference filter, or with the monochromated (390 nm) light from a Xe lamp. PL spectra were measured with a cooled Oriel Instaspec IV spectrograph combined with a CCD detector. Fibers for X-ray scattering were drawn from a liquid-crystalline melt. The viscosity was adjusted by moving a glass slide with molten sample on the working surface of a "System Kofler" temperature gradient bar. Fiber drawing shear aligns the LC domains parallel to the fiber axis, and since the thin fiber rapidly cools in ambient air, the aligned LC is quenched into a glassy state. For X-ray diffraction, fibers were irradiated with pinhole-colliminated graphite-monochromatized Cu Kα X-rays, and diffraction patterns were collected with a MarResearch 2-dimensional image-plate detector. A homemade temperature-controlled cell was used, and the beam path up to the beam stop was enclosed in a helium-flushed tent. Cerius-2 software was used for molecular modeling.

Acknowledgment. We gratefully acknowledge the UK Engineering and Physical Sciences Research Council for funding the work in Sheffield through Grant GR/M08011 and via a studentship to K.S.W. We thank Ed Woo and Mike Inbasekaran and The Dow Chemical Co. for providing the samples of PFO. We also thank Peter Raynes and Andy Hudson of Sharp Laboratories of Europe for their helpful contributions to this work. Finally, we thank Mike Turner, Ullrich Scherf, Gerhard Wegner, David Lidzey, Helen Mellor, and Dieter Neher for useful discussions.

References and Notes

(1) Burroughes, J. H.; Bradley, D. D. C.; Brown, A. R.; Marks, R. N.; Mackay, K.; Friend, R. H.; Burn, P. L.; Holmes, A. B. *Nature* **1990**, *347*, 539.

(2) Bradley, D. D. C. *Curr. Opin. Solid State Mater. Sci.* **1996**, *1*, 789. Salbeck, J. *Ber. Bunsen-Ges. Phys. Chem*. **1996**, *100*, 1666. Kraft, A.; Grimsdale, A. C.; Holmes, A. B. *Angew. Chem., Int. Ed. Engl.* **1998**, *37*, 402. Sixl, H.; Schenk, H.; Yu, N. *Phys. Bl.* **1998**, *54*, 225. Greiner, A. *Polym. Adv. Technol.* **1998**, *9*, 371. Friend, R. H.; Gymer, R. W.; Holmes, A. B.; Burroughes, J. H.; Marks, R. N.; Taliani, C.; Bradley, D. D. C.; Dos Santos, D. A.; Brédas, J. L.; Löglund, M.; Salaneck, W. R. *Nature* **1999**, *397*, 121.

(3) Hörhold, H. H.; Helbig, M.; Raabe, D.; Opfermann, J.; Scherf, U.; Stockmann, R.; Weiss, D. *Z. Chem*. **1987**, *27*, 126.

(4) Spreitzer, H.; Becker, H.; Kluge, E.; Kreuder, W.; Schenk, H.; Demandt, R.; Schoo, H. *Adv. Mater.* **1998**, *10*, 1340.

(5) (a) Woo, E. P.; Inbasekaran, M.; Shiang, W.; Roof, G. R. Int. Pat. Appl. WO 97/05184, 1995. (b) Inbasekaran, M.; Wu, W.; Woo, E. P. US Pat. 5,777,070, 1998.

(6) Redecker, M.; Bradley, D. D. C.; Inbasekaran, M.; Woo, E. P. *Appl. Phys. Lett*. **1998**, *73*, 1565.

(7) Grice, A.; Bradley, D. D. C.; Bernius, M. T.; Inbasekaran, M.; Wu, W. W.; Woo, E. P. *Appl. Phys. Lett.* **1998**, *73*, 629.
(8) Yang, Y.; Pei, Q. *Polym. Prepr.* **1997**, *38*, 335.
(9) Ranger, M.; Leclerc, M. *Can. J. Chem.* **1999**, *76*, 1571.
(10) Grell, M.; Redecker, M.; Whitehead, K. S.; Bradley, D. D. C.; Inbasekaran, M.; Woo, E. P.; Wu, W. *Liq. Cryst.*, in press.
(11) Grell, M.; Bradley, D. D. C.; Inbasekaran, M.; Woo, E. P. *Adv. Mater.* **1997**, *9*, 798.
(12) Schartel, B.; Wachtendorf, V.; Grell, M.; Bradley, D. D. C.; Hennecke, M. *Phys. Rev. B* **1999**, *60*, 277.
(13) Grell, M.; Knoll, W.; Lupo, D.; Meisel, A.; Miteva, T.; Neher, D.; Nothofer, H. G.; Scherf, U.; Yasuda, A. *Adv. Mater.* **1999**, *11*, 671.
(14) Grell, M.; Bradley, D. D. C., *Adv. Mater.*, in press.
(15) Bradley, D. D. C.; Grell, M.; Long, X.; Mellor, H.; Grice, A. *Proc. SPIE* **1997**, *3145*, 254.
(16) Grell, M.; Bradley, D. D. C.; Long, X.; Chamberlain, T.; Inbasekaran, M.; Woo, E. P.; Soliman, M. *Acta Polym.* **1998**, *49*, 439.
(17) Klärner, G.; Miller, R. D. *Macromolecules* **1998**, *31*, 2007.
(18) Janietz, S.; Bradley, D. D. C.; Grell, M.; Giebeler, C.; Inbasekaran, M.; Woo, E. P. *Appl. Phys. Lett.* **1998**, *73*, 2453.
(19) Kreyenschmidt, M.; Klärner, G.; Fuhrer, T.; Ashenhurst, J.; Karg, S.; Chen, W. D.; Lee, V. Y.; Scott, J. C.; Miller, R. D. *Macromolecules* **1998**, *31*, 1099.
(20) Klärner, G.; Davey, M. H.; Chen, W. D.; Scott, J. C.; Miller, R. D. *Adv. Mater.* **1998**, *10*, 993.
(21) Ranger, M.; Rondeau, D.; Leclerc, M. *Macromolecules* **1997**, *30*, 7686.
(22) Ranger, M.; Leclerc, M. *Synth. Met.*, in press.
(23) Lemmer, U.; Heun, S.; Mahrt, R. F.; Scherf, U.; Hopmeier, M.; Siegner, U.; Göbel, E. O.; Müllen, K.; Bässler, H. *Chem. Phys. Lett.* **1995**, *240*, 373.
(24) Halkyard, C. E.; Rampey, M. E.; Kloppenburg, L.; Studer-Martinez, S. L.; Bunz, U. H. F. *Macromolecules* **1998**, *31*, 8655.
(25) Bliznyuk, V. N.; Carter, S. A.; Scott, J. C.; Klärner, G.; Miller, R. D.; Miller, D. C. *Macromolecules* **1999**, *32*, 361.
(26) Yan, M.; Rothberg, L. J.; Papadimitrakopoulos, F.; Galvin, M. E.; Miller, T. M. *Phys. Rev. Lett.* **1994**, *73*, 744.
(27) Brandrup, J., Immergut, J. H., Eds. *Polymer Handbook*; Wiley: New York, 1975.
(28) Blatchford, J. W.; Jessen, S. W.; Lin, L. B.; Gustafson, T. L.; Fu, D. K.; Wang, H. L.; Swager, T. M.; MacDiarmid, A. G.; Epstein, A. J. *Phys. Rev. B* **1996**, *54*, 9180.
(29) Mahrt, R. F.; Pauck, T.; Lemmer, U.; Siegener, U.; Hopmeier, M.; Hennig, R.; Bässler, H.; Göbel, E. O.; Haring-Bolivar, P.; Wegmann, G.; Kurz, H.; Scherf, U.; Müllen, K. *Phys. Rev. B* **1996**, *54*, 1759.
(30) Hertel, D.; Scherf, U.; Bässler, H. *Adv. Mater.* **1998**, *10*, 1119.
(31) Flory, P. J. *Principles of Polymer Chemistry*; Cornell University Press: Ithaca, NY, 1953; p 577.
(32) Pasco, S. T.; Baker, G. L. *Synth. Met.* **1997**, *84*, 275.
(33) Atkins, P. W. *Physical Chemistry*, 5th ed.; Oxford University Press: New York, 1995; p 283.
(34) Saiani, A.; Spèvacek, J.; Guenet, J. M. *Macromolecules* **1998**, *31*, 703.
(35) Berghmans, M.; Thijs, S.; Cornette, M.; Berghmans, H.; de Schryver, F. C.; Moldenaers, P.; Mewis, J. *Macromolecules* **1994**, *27*, 7669.
(36) Berghmans, H.; Donkers, A.; Frenay, L.; Stoks, W.; de Schryver, F. C.; Moldenaers, P.; Mewis, J. *Polymer* **1987**, *28*, 97.
(37) Klug, H.; Alexander, L. B. *X-ray Diffraction Procedures for Polycrystalline and Amorphous Materials*, 2nd ed.; Wiley: New York, 1979.
(38) (a) M Ballauf, M. *Angew. Chem.* **1989**, *101*, 261. (b) Neher, D. *Adv. Mater.* **1995**, *7*, 691.
(39) Ezquerra, A.; Sanchez-Cuesta, M.; Ungar, G.; Feijoo, J. L.; Lopez-Cabarcos, E. *J. Polym. Sci., Polym. Phys.* **1998**, *36*, 49−54.
(40) Hosemann, R.; Bagchi, S. N. *Direct Analysis of Diffraction by Matter*; North-Holland: Amsterdam, 1962.
(41) Bradley, D. D. C.; Grell, M.; Grice, A. W.; Tajbakhsh, A. R.; O'Brien, D. F.; Bleyer, A. *Opt. Mater.* **1998**, *9*, 1. O'Brien, D. F.; Bleyer, A.; Lidzey, D. G.; Bradley, D. D. C.; Tsutsui, T. *J. Appl. Phys.* **1997**, *82*, 2662.
(42) Heun, S.; Mahrt, R. F.; Greiner, A.; Lemmer, U.; Bässler, H.; Halliday, D. A.; Bradley, D. D. C.; Burn, P. L.; Holmes, A. B. *J. Phys: Condens. Matter* **1993**, *5*, 247.

MA990741O